Earth Syst. Sci. Data Discuss., 7, 129–148, 2014
www.earth-syst-sci-data-discuss.net/7/129/2014/
doi:10.5194/essdd-7-129-2014

Open Access Earth System Science Data Discussions

High-resolution ice thickness and bed topography of a land-terminating section of the Greenland Ice Sheet

K. Lindbäck[1], R. Pettersson[1], S. H. Doyle[2], C. Helanow[3], P. Jansson[3], S. Savstrup Kristensen[4], L. Stenseng[4], R. Forsberg[4], and A. L. Hubbard[2]

[1]Department of Earth Sciences, Air, Water, and Landscape Sciences, Uppsala University, Villavägen 16, 752 36 Uppsala, Sweden
[2]Department of Geography and Earth Sciences, Aberystwyth University, Llandinam Building Penglais Campus, Aberystwyth SY23 3DB, UK
[3]Department of Physical Geography and Quaternary Geology, Stockholm University, Svante Arrhenius väg 8, 106 91 Stockholm, Sweden
[4]Technical University of Denmark, National Space Institute, Elektrovej, Buildning 327, 2800 Lyngby, Denmark

Received: 24 February 2014 – Accepted: 17 March 2014 – Published: 26 March 2014

Correspondence to: K. Lindbäck (katrin.lindback@geo.uu.se)

Published by Copernicus Publications.

Abstract

We present ice thickness and bed topography maps with high spatial resolution (250 to 500 m) of a land-terminating section of the Greenland Ice Sheet derived from combined ground-based and airborne radar surveys. The data have a total area of ~ 12 000 km^2 and cover the whole ablation area of the outlet glaciers of Isunnguata Sermia, Russell, Leverett, Ørkendalen and Isorlersuup up to the long-term mass balance equilibrium line altitude at ~ 1600 m above sea level. The bed topography shows highly variable subglacial trough systems, and the trough of the Isunnguata Sermia Glacier is over-deepened and reaches an elevation of several hundreds of meters below sea level. The ice surface is smooth and only reflects the bedrock topography in a subtle way, resulting in a highly variable ice thickness. The southern part of our study area consists of higher bed elevations compared to the northern part. The covered area is one of the most studied regions of the Greenland Ice Sheet with studies of mass balance, dynamics, and supraglacial lakes, and our combined dataset can be valuable for detailed studies of ice sheet dynamics and hydrology. The compiled datasets of ground-based and airborne radar surveys are accessible for reviewers (password protected) at doi.pangaea.de/10.1594/pangaea.830314 and will be freely available in the final revised paper.

1 Introduction

The first radar measurements on the Greenland Ice Sheet were collected in the 1960's (Evans, 1963; Waite and Schmidt, 1962). Since then, various campaigns have measured the elevation of the ice-covered bedrock (Bogorodsky et al., 1985; Evans and Robin, 1966; Letreguilly et al., 1991). The first compilation of bed elevation data over the whole Greenland ice sheet by Bamber et al. (2001) consisted of 5 km gridded maps of ice thickness and bed topography. Numerous surveys have increased the density, or

ESSDD
7, 129–148, 2014

filled gaps, in this grid and an updated bed map, with six different data sources, was recently published as a 1 km grid (Bamber et al., 2013a).

The size of many outlet glaciers in Greenland is small and bed elevation datasets with a higher resolution than is currently available are required for modelling of ice sheet dynamics. On a regional scale, high resolution DEMs of the bed also allow subglacial hydrological pathways and drainage basins to be determined with confidence (e.g. Wingham et al., 2006; Wright et al., 2008) and subglacial landforms and landscapes to be studied in detail (e.g. Bamber et al., 2013b; Bingham and Siegert, 2009; King et al., 2009). Recent high resolution measurements of ice thickness have focused on mapping the fast-flowing marine-terminating glaciers (e.g. Plummer et al., 2008; Raney, 2009) that drain the majority of the Greenland Ice Sheet, while the typically slower, land-terminating glaciers have received less attention. Land-terminating glaciers and their catchments, however, provide ideal study areas for investigating the response of ice sheet dynamics to atmospheric forcing, as they are isolated from marine-influences such as calving and submarine melt. Furthermore, under a warming climate tidewater outlet glaciers are expected to retreat inland, causing a larger portion of the ice sheet to be land-terminating in the future (Sole et al., 2008). A higher resolution bed map (< 1 km grid) of a land-terminating region of the Greenland Ice Sheet is therefore timely.

Here, we present ice thickness and bed topography DEMs of a land-terminating section of the Greenland Ice Sheet, based on a compilation of ground-based and airborne radar surveys. The DEMs have a total area of $\sim 12\,000\,\text{km}^2$ at a resolution of 250 to 500 m. Our combined dataset of ground-based and airborne radar surveys is available for integration into databases of bed elevation on Greenland (e.g. Bamber et al., 2013a) and can be valuable for detailed studies of ice sheet dynamics and hydrology. Our collected data will be used in a project that aim to improve the current understanding of hydrogeological processes associated with continental-scale glacial periods, including the presence of permafrost and the advance/retreat of ice sheets.

1.1 Study area

The study area is located in West Greenland and includes the officially unnamed Isunnguata Sermia, Russell, Leverett, Ørkendalen and Isorlersuup outlet glaciers and their catchment areas. The radar survey extends a further 100 km south of the Isorlersuup Glacier and 90 km inland to approximately the 21 year-mean mass balance equilibrium line altitude (ELA) at ~ 1553 m above sea level (a.s.l.) (van de Wal et al., 2012). The glaciated area is one of the most studied regions of the Greenland Ice Sheet with studies of mass balance (e.g. van de Wal et al., 2012), dynamics (e.g. van de Wal et al., 2008; Bartholomew et al., 2011; Palmer et al., 2011; Sole et al., 2013), and supraglacial lakes (Doyle et al., 2013; Fitzpatrick et al., 2014). Recently, two studies have published DEMs of Isunnguata Sermia and Russell Glacier (Jezek et al., 2013; Morlighem et al., 2013), based on the IceBridge dataset (Leuschen and Allen, 2010), also used in this study (see Sect. 2.2). These studies cover the northern part of our subglacial area, to an extent of ~ 25 % of our maps. In comparison, our data cover the whole ablation area and contain, in addition to the IceBridge dataset, two previously unpublished datasets.

2 Data and methods

The dataset in this study was compiled from three different sources (Fig. 1). We collected ground-based radar surveys during spring 2010 and spring 2011 which we combined with two airborne radar datasets, collected by the Technical University of Denmark in 2003 (previously unpublished) and by the NASA IceBridge project between 2010 and 2012 (Leuschen and Allen, 2010). In the following sections, we describe the methods used to acquire each dataset, how these datasets were assimilated and interpolated into the final data product. The system parameters of each dataset are summarised in Table 1.

ESSDD
7, 129–148, 2014

2.1 Ground-based radar surveys

During spring (April to May) in 2010 and 2011 we collected ~ 1500 km of common-offset radar profiles with two ground-based impulse radar systems, hereafter referred to as the UU (Uppsala University) dataset. Each radar system consisted of resistively loaded half-wavelength dipole antennas of 2.5 MHz centre frequency. An impulse transmitter was used with an average output power of 35 W and a pulse repetition frequency of 1 kHz. The 16-bit receiver had a bandwidth of 200 MHz and a capacity of collecting ~ 5000 traces per second. The trace acquisition was triggered by the direct wave between transmitter and receiver. We towed the radar systems with snowmobiles at ~ 10 km h^{-1}, along tracks separated by 2 km. By stacking 3000 traces we achieved a trace spacing of ~ 15 m. Trace positioning was achieved using data from a dual-frequency GPS receiver located by the radar receiver. The GPS data were processed kinematically using the Canadian Reference System's precise point positioning service (Natural Resources Canada, 2013), which has an estimated theoretical uncertainty of ±0.02 m in the horizontal and ±0.03 m in the vertical. In practice, however, an error of ±1 m in the surface elevation is expected due to the placement of the antenna relative the common midpoint of the radar.

We applied several corrections and filters to the radar data: (1) a butterworth band-pass filter, with cut-off frequencies of 0.75 MHz and 7 MHz, was used to remove the unwanted frequency components in the data; (2) normal move-out correction was applied to correct for antenna separation; (3) rubber-band correction was used to interpolate the data to uniform trace spacing; and (4) 2-D frequency wavenumber migration (Stolt, 1978) was used to collapse hyperbolic reflectors back to their original positions in the profile direction. The bed returns were digitized semi-automatically with a cross-correlation picker (Irving et al., 2007). We calculated the ice thickness from the picked travel-times of the bed return using a constant radar signal speed of 168 m μs^{-1} (discussed further in Sect. 2.3.1). Figure 2 shows an example image of a processed radar profile.

ESSDD
7, 129–148, 2014

2.2 Airborne radar surveys

In addition to the ground-based data, we used two other datasets of subglacial topography provided by the Technical University of Denmark and NASA's IceBridge project, hereafter referred to as the DTU and IceBridge datasets. There are also data in the area collected by the Center for Remote Sensing of Ice Sheets (CReSIS) between 1993 and 2009 (Gogineni et al., 2001), but we decided not to include this data as they had a lower resolution and provided no significant extended coverage.

The DTU dataset in our study area consists of ~ 3000 km of airborne radar profiles collected using a 60 MHz pulse radar during 2003. Data acquisition took place along flight tracks separated by ~ 2.5 km, with a sampling rate of 3.125 Hz giving an along-track sample spacing of ~ 25 m after processing (Christensen et al., 2000). Laser altimetry measurements of ice surface elevation allowed ice thickness to be determined (Forsberg et al., 2001). A southern subset of the DTU dataset was published by Ahlstrøm et al. (2005).

The IceBridge dataset in our study area consists of ~ 5500 km of airborne radar data, with a centre frequency of 194 MHz, collected between 2010 and 2012 along flight tracks, with a data trace spacing of ~ 15 m, separated by ~ 500 m in the densely-surveyed northern region (Fig. 1). Several processing steps were applied to produce echograms as described by Leuschen and Allen (2010), including synthetic aperture radar (SAR) processing. Using a combination of echograms, the ice surface and bed layers were identified and the ice thickness was calculated by subtracting the bed layer from the surface layer. The layer tracking of the reflectors were done manually with basic tools for partial automation (e.g. automatic peak detector).

2.3 Radar system errors and uncertainty

The datasets were collected using different radar systems with varying specifications, and as a result they have varying vertical and horizontal resolutions.

ESSDD
7, 129–148, 2014

2.3.1 Vertical resolution

The range resolution is the accuracy of the distance between the antenna and the bed and can be determined by the characteristics of the source pulse (i.e., bandwidth) and the digitization frequency. We estimated that the system errors for the UU dataset are 18.8 m based on receiver and transmitter characteristics. The DTU dataset has a range resolution of ∼ 21 m, but the resolution can be significantly better if the signal-to-noise ratio is large (Christensen et al., 2000). The IceBridge dataset has an along-track range resolution of 4.5 m (Leuschen and Allen, 2010). The use of a constant signal velocity (168 $m\,\mu s^{-1}$ in our case) for the ground-based and airborne surveys is a common method within glaciology, since glacial ice can be assumed to be a homogenous medium (e.g. Lythe et al., 2001). The wave speed, however, can vary spatially depending on mainly density, for example with the presence of a firn layer. The profiles were collected in the ablation zone with thin seasonal snow cover; thus we assume small density variations due to impurities in the ice (i.e., air bubbles). A typical variation of 2 % of glacier ice density (Navarro and Eisen, 2009) gives an uncertainty of ±20 m on the depth conversion (with an ice depth of 1000 m). The velocity of the radar signal can also vary because of inhomogeneities, ice temperature, and presence of liquid water in the ice (Drewry, 1975). The effect of inhomogeneities and ice temperature is expected to have a small impact on the average velocity for the whole ice column while a significant water content in the ice can influence the velocity in a substantial way. In most parts of the study area, however, only the basal layer (< 10 % of the total thickness) is temperate and allow for liquid water, which would give an underestimation of ∼ 0.7 % of the average velocity at 2 % water content. Errors can also arise when processing the radar signal, since the bed was identified semi-automatically as a reflector on the radar image (Fig. 2).

To estimate picking and positioning errors within each dataset and to test the consistency between the datasets we compared the differences (misfits) in the ice thickness and surface elevation estimates between different profiles and datasets at crossover

ESSDD
7, 129–148, 2014

points. The UU dataset had a mean crossover misfit in ice thickness of 16.0 m with a standard deviation σ of 20.3 m (based on 159 crossing points). The mean crossover misfit in ice surface elevation was 0.6 ($\sigma = 0.9$ m). The DTU dataset had a mean crossover misfit in ice thickness of 12.0 m with a standard deviation of 13.0 m (based on 97 crossing points). The mean crossover misfit in ice surface elevation was 8.7 m ($\sigma = 11.3$ m). The IceBridge dataset had a mean crossover misfit in ice thickness of 18.9 m with a standard deviation of 26.8 m (based on 1909 crossing points). The mean crossover misfit in surface elevation was 11.3 m ($\sigma = 15.9$ m). As the crossover analysis within the same dataset does not capture systematic errors between the different datasets, and since ten years (2003 to 2012) separate the data acquisition, a comparison between the datasets is essential. When we ran a crossover analysis between the datasets there was a mean misfit in ice thickness of 19.7 m ($\sigma = 24.6$ m). The mean crossover misfit in surface elevation of all the datasets was 8.1 m ($\sigma = 7.5$ m). With the inherited accuracy of the radar signal (system specifications and 2 % difference in signal velocity), we estimated the total root-mean-squared uncertainty of the ice thickness to be 18.3 m for UU dataset, 18.1 m for the DTU dataset, and 16.1 m for the IceBridge dataset.

2.3.2 Horizontal resolution

Since the antenna footprint is large, echoes from a large area at the bed will be integrated into the signal both along-track and across-track, and therefore the horizontal resolution will be determined by the range resolution. The horizontal resolution is also dependent on the vertical variation (roughness) of the bed within the footprint and the errors can be large since the topography and acquisition geometry is, by necessity, not ideal. Theoretically, the reflected energy does not arrive at the receiver from a single point, but from an ellipsoidal zone of a horizontal plane, called the first Fresnel zone (Robin et al., 1969). Given an ice thickness of 1000 m, the first Fresnel zone is 183 m for the UU dataset. This is only a theoretical resolution and is improved by the applied 2-D migration along the profiles, which collapses hyperbolic reflectors back to their original position. The post-migration resolution is $\lambda/2$, where λ is the wavelength of the radar signal at the centre frequency (Welch et al., 1998). Since $\lambda = v/f$, where v is the signal velocity and f is the frequency, the theoretical minimal resolution is 34 m for the UU dataset (f = 2.5 MHz). This is, however, only valid in the travel direction and does not account for diffraction orthogonal to the profiles. Therefore, large errors in the thickness measurements can still be expected in areas with steep slopes perpendicular to the direction of the profiles. The ideal measuring technique in such cases is 3-D migration, however, this could not be applied since this requires a shorter distance between the profiles to avoid aliasing. The DTU dataset has not been migrated and has an expected along-track and across-track resolution of 81 m (Christensen et al., 2000). The IceBridge dataset has an along-track resolution of 25 m and across-track resolution of 323 m for smooth terrain and 651 m for rough terrain, where the ice thickness is 2000 m and height above the air/ice interface is 500 m (Leuschen and Allen, 2010).

2.4 Assimilation of the datasets

We combined the ground-based and airborne datasets to produce DEMs of ice thickness and bed topography. The datasets are dense along the profiles, with a data point spacing of 15 to 25 m, compared with 500 to 2500 m spacing between individual profiles. As this non-uniform spacing is not optimal for gridding algorithms, we sub-gridded the ground-based and airborne datasets into a 100 m pseudo-grid to reduce the data density along individual profiles. The sub-grid was produced by calculating the median values for the points that fell within the distance of half the grid cell. Before we interpolated the ice thickness data, we added zero ice thickness along the edge of the ice sheet, which we derived from SPOT-5 satellite images acquired in August 2008. We interpolated the sub-gridded profiles to 250 m resolution in the northern part of the study area (above 66.7° N), where there was high spatial density of profiles, and to 500 m resolution in the southern part (below 66.7° N), where the spacing between profiles was the largest. We used an universal kriging interpolation algorithm (e.g. Isaaks and Srivastava, 1989) with a linear drift applied to remove large-scale trends. The interpolation

ESSDD
7, 129–148, 2014

model was based on an anisotropic variogram model, with linear and exponential models representing the spatial variability of the dataset. We applied a smoothing nugget effect of 20 m to account for the accuracy of the data points.

We calculated the bed elevation by subtracting the ice thickness from the surface elevation in every grid point. For surface elevation we used the Greenland Ice Sheet Mapping Project (GIMP) surface elevation model (Howat et al., 2014). The GIMP surface elevation model is constructed from a combination of ASTER and SPOT-5 DEM's for the peripheral areas of the ice sheet, with a horizontal resolution of 30 m. The root-mean-squared validation error, relative to ICESat, is ±10 m for the GIMP dataset. We constructed the bed topography dataset in this way, instead of using the surface elevation data collected during the radar surveys, to give the compiled dataset the same surface reference. To assure that this is a valid step, since the datasets were collected in different years (between 2003 and 2012), we subtracted the GIMP surface elevation at every dataset surface elevation point. The mean difference between the surfaces was calculated to be −5 m with a standard deviation of 10 m.

To assess the error in interpolation we cross-validated the gridded data; this is a common validation technique to see how well a model fits the observed data. By removing one observation from the dataset, the remaining data were used to interpolate a value for the removed observation. This process was continued for 1000 random observations in the data; the error is the residual between the observed and the interpolated value (Isaaks and Srivastava, 1989). The standard deviation of the residuals was estimated to be 17 m, and increases with distance from the profiles (Fig. 3a). The data are missing in some sections of the tracks, primarily close to the ice margin (∼ 0 to 20 km; Fig. 3a), where it was difficult to receive a bed signal through fractured ice.

To summarise, the total accuracy of the estimated ice thickness and bed topography dependent on: (i) the technical and theoretical capability of the radar systems; (ii) uncertainty in the depth conversion; and (iii) picking, positioning, and interpolation errors. By assessing all these potential sources of error, we estimate the maximum vertical root-mean-squared uncertainty in the final interpolated DEMs to be approximately 20 m.

3 Results

We present DEMs of ice thickness and bed topography of a land-terminating section of the Greenland Ice Sheet at a 250 to 500 m spatial resolution (Fig. 3c and d). Due to a smooth ice surface and an undulating bed the ice thickness is highly variable (Fig. 3c), with a maximum gridded ice depth of 1460 m and a mean value of 830 m. Consistent with previous studies (e.g. Budd and Carter, 1971; Gudmundsson, 2003) the surface has a secondary component that is a subtle expression of the basal topography. The ice flow direction in the area generally runs from east to west, with a mean surface velocity of $\sim 150\,\mathrm{m\,yr^{-1}}$ (Fig. 3b; Joughin et al., 2010).

The highly variable subglacial topography (Fig. 3d) resembles the landscape in front of the ice sheet. The bed topography gets smoother away from the ice margin, consistent with the larger, but lower resolution, bed map of Greenland (Bamber et al., 2013a). The deepest trough lies under the Isunnguata Sermia Glacier and has a minimum gridded elevation of −510 m below the WGS-1984 ellipsoid (−540 m in the raw data) with a maximum difference of ∼ 1000 m between the valley bottom and adjacent subglacial hills. The southern part of the dataset (south of 66.7° N) consists of an area with higher bed elevations and includes the highest subglacial peak of 1060 m above the WGS-1984 ellipsoid (1100 m in the raw data). In comparison with the Bamber et al. (2013a) bed DEM, our data show a mean difference in elevation of 82 m (σ = 105 m). The relative large difference between the two DEMs is possibly caused by our higher data density and higher gridded spatial resolution which creates larger detail in the DEMs. In addition, our interpolation model has been optimized for the region compared to the whole Greenland Ice Sheet. This highlights the need for regionally optimized DEMs when conducting detailed studies of the Greenland Ice Sheet.

ESSDD
7, 129–148, 2014

4 Summary and outlook

We have compiled ground-based and airborne radar surveys from various sources to produce ice thickness and bed topography DEMs with high spatial resolution (250 to 500 m) of a land-terminating section of the western Greenland Ice Sheet. The DEMs cover the whole ablation area (12 000 km^2) up to the long term ELA at ~ 1600 m a.s.l., 90 km inland. The bed topography shows highly variable subglacial trough systems, resembling the landscape in the proglacial area. The ice surface is smooth and only reflects the bedrock topography in a subtle way, resulting in a highly variable ice thickness. The southern part of our study area consists of higher bed elevations compared to the northern part.

Further improvement of our maps could include filling in the gaps in the ice thickness and bed topography maps, by surveying parts of the ice margin that are highly crevassed. This would demand a low-frequency airborne radar system designed for warm and fractured ice. Surveying the area with 3-D radar tomography (e.g. Paden et al., 2010) would also increase the spatial resolution substantially. Our maps, nevertheless, contain enough detail for a wide range of studies and can contribute to improvements in future ice sheet modelling efforts and studies of ice sheet dynamics and hydrology. The compiled datasets of ground-based and airborne radar surveys are accessible for reviewers (password protected) at doi.pangaea.de/10.1594/pangaea.830314 and will be freely available in the final revised paper.

Supplementary material related to this article is available online at http://www.earth-syst-sci-data-discuss.net/7/129/2014/essdd-7-129-2014-supplement.zip.

Acknowledgements. This project was funded by the Greenland Analogue Project (GAP), a collaborative project funded by the nuclear waste management organizations in Sweden (Svensk Kärnbränslehantering AB), Finland (Posiva Oy) and Canada (NWMO). The objective of the

ESSDD
7, 129–148, 2014

project is to improve our current understanding of how long-term geological repositories for spent nuclear fuel are influenced by future glacial cycles. Field support was also given from the Swedish Society for Anthropology and Geography (SSAG) and the Geographical Society of Uppsala. We would also like to thank Dirk van As and Heidi Sevestre for assistance in the field. SPOT images were provided by the SPIRIT Program© CNES 2008–2009 and SPOT Image 2008.

References

Ahlstrøm, A. P., Mohr, J. J., Reeh, N., Christensen, E. L., and Hooke, R. L.: Controls on the basal water pressure in subglacial channels near the margin of the Greenland ice sheet, J. Glaciol., 51, 443–450, doi:10.3189/172756505781829214, 2005.

Bamber, J. L., Ekholm, S., and Krabrill, W.: A new, high-resolution digital elevation model of Greenland fully validated with airborne laser altimeter data, J. Geophys. Res., 106, 6733–6745, 2001.

Bamber, J. L., Griggs, J. A., Hurkmans, R. T. W. L., Dowdeswell, J. A., Gogineni, S. P., Howat, I., Mouginot, J., Paden, J., Palmer, S., Rignot, E., and Steinhage, D.: A new bed elevation dataset for Greenland, The Cryosphere, 7, 499–510, doi:10.5194/tc-7-499-2013, 2013a.

Bamber, J. L., Siegert, M. J., Griggs, J. A., Marshall, S. J., and Spada, G.: Paleofluvial Mega-Canyon Beneath the Central Greenland Ice Sheet, Science, 341, 997–999, doi:10.1126/science.1239794, 2013b.

Bartholomew, I. D., Nienow, P., Sole, A., Mair, D., Cowton, T., King, M. A., and Palmer, S.: Seasonal variations in Greenland Ice Sheet motion: Inland extent and behaviour at higher elevations, Earth Planet. Sc. Lett., 307, 271–278, doi:10.1016/j.epsl.2011.04.014, 2011.

Bingham, R. G. and Siegert, M. J.: Quantifying subglacial bed roughness in Antarctica: implications for ice-sheet dynamics and history, Quaternary Sci. Rev., 28, 223–236, doi:10.1016/j.quascirev.2008.10.014, 2009.

Bogorodsky, V., Bentley, C., and Gudmandsen, P.: Radioglaciology, Reidel, Dordrecht, 1985.

Budd, W. F. and Carter, D. B.: An analysis of the relation between the surface and bedrock profiles of ice caps, J. Glaciol., 10, 197–209, 1971.

Christensen, E. L., Reeh, N., Forsberg, R., Jørgensen, J. H., Skou, N., and Woelders, K.: Instruments and methods: a low-cost glacier-mapping system, J. Glaciol., 46, 531–537, 2000.

ESSDD
7, 129–148, 2014

Doyle, S. H., Hubbard, A. L., Dow, C. F., Jones, G. A., Fitzpatrick, A., Gusmeroli, A., Kulessa, B., Lindback, K., Pettersson, R., and Box, J. E.: Ice tectonic deformation during the rapid in situ drainage of a supraglacial lake on the Greenland Ice Sheet, The Cryosphere, 7, 129–140, doi:10.5194/tc-7-129-2013, 2013.

Drewry, D.: Comparison of electromagnetic and seismic-gravity ice thickness measurements in East Antarctica, J. Glaciol., 15, 137–150, 1975.

Evans, S.: International co-operative field experiments in glacier sounding, Greenland, Polar Rec., 11, 725–726, 1963.

Evans, S. and Robin, G.: Glacier depth-sounding from the air, Nature, 210, 883–885, 1966.

Fitzpatrick, A. A. W., Hubbard, A. L., Box, J. E., Quincey, D. J., van As, D., Mikkelsen, A. P. B., Doyle, S. H., Dow, C. F., Hasholt, B., and Jones, G. A.: A decade (2002–2012) of supraglacial lake volume estimates across Russell Glacier, West Greenland, The Cryosphere, 8, 107–121, doi:10.5194/tc-8-107-2014, 2014.

Forsberg, R., Keller, K., and Jacobsen, S. M.: Laser monitoring of ice elevations and sea-ice thickness in Greenland, Int. Arch. Photogramm. Remote Sens., XXXIV, 163–168, 2001.

Gogineni, S., Tammana, D., Braaten, D., Leuschen, C., Akins, T., Legarsky, J., Kanagaratnam, P., Stiles, J., Allen, C., and Jezek, K.: Coherent radar ice thickness measurements over the Greenland ice sheet, J. Geophys. Res., 106, 33761–33772, 2001.

Gudmundsson, G. H.: Transmission of basal variability to a glacier surface, J. Geophys. Res., 108, B52253, doi:10.1029/2002JB002107, 2003.

Howat, I. M., Negrete, A., and Smith, B. E.: The Greenland Ice Mapping Project (GIMP) land classification and surface elevation datasets, The Cryosphere Discuss., 8, 453–478, doi:10.5194/tcd-8-453-2014, 2014.

Irving, J. D., Knoll, M. D., and Knight, R. J.: Improving crosshole radar velocity tomograms: A new approach to incorporating high-angle traveltime data, Geophysics, 72, 31–41, doi:10.1190/1.2742813, 2007.

Isaaks, E. H. and Srivastava, R. M.: An Introduction to Applied Geostatistics, Oxford University Press, New York, 1989.

Jezek, K., Wu, X., Paden, J., and Leuschen, C.: Radar mapping of Isunguata Sermia, Greenland, J. Glaciol., 59, 1135–1146, doi:10.3189/2013JoG12J248, 2013.

Joughin, I., Smith, B. E., Howat, I. M., Scambos, T., and Moon, T.: Greenland flow variability from ice-sheet-wide velocity mapping, J. Glaciol., 56, 415–430, doi:10.3189/002214310792447734, 2010.

Discussion Paper | Discussion Paper | Discussion Paper | Discussion Paper |

King, E. C., Hindmarsh, R. C. A., and Stokes, C. R.: Formation of mega-scale glacial lineations observed beneath a West Antarctic ice stream, Nat. Geosci., 2, 585–588, doi:10.1038/ngeo581, 2009.

Letreguilly, A., Huybrechts, P., and Reeh, N.: Steady-state characteristics of the Greenland ice sheet under different climates, J. Glaciol., 37, 149–157, 1991.

Leuschen, C. and Allen, C.: IceBridge MCoRDS L2 Ice Thickness, 2010–2012, Boulder, Colorado, USA NASA DAAC Natl. Snow Ice Data Cent, available at: http://nsidc.org/data/irmcr2.htm (last access: 10 January 2013), 2010.

Lythe, M. B., Vaughan, D. G., and the BEDMAP Consortium: BEDMAP: A new ice thickness and subglacial topographic model of Antarctica, J. Geophys. Res., 106, 11335–11351, 2001.

Morlighem, M., Rignot, E., Mouginot, J., Wu, X., Seroussi, H., Larour, E., and Paden, J.: High-resolution bed topography mapping of Russell Glacier, Greenland, inferred from Operation IceBridge data, J. Glaciol., 59, 1015–1023, doi:10.3189/2013JoG12J235, 2013.

Natural Resources Canada: CSRS-PPP: On-Line GNSS PPP Post-Processing Service, available at: http://webapp.geod.nrcan.gc.ca/geod/tools-outils/ppp.php (last access: 10 January 2013), 2013.

Navarro, F. J. and Eisen, O.: Ground penetrating radar, in: Remote Sensing of Glaciers – Techniques for Topographic, Spatial and Thematic Mapping, edited by: Pellikka, P. and Rees, W. G., Taylor & Francis group, London, 195–229, 2009.

Paden, J., Akins, T., Dunson, D., Allen, C., and Gogineni, P.: Ice-sheet bed 3-D tomography, J. Glaciol., 56, 3–11, doi:10.3189/002214310791190811, 2010.

Palmer, S., Shepherd, A., Nienow, P., and Joughin, I.: Seasonal speedup of the Greenland Ice Sheet linked to routing of surface water, Earth Planet. Sc. Lett., 302, 423–428, doi:10.1016/j.epsl.2010.12.037, 2011.

Plummer, J., Gogineni, S., van der Veen, C., Leuschen, C., and Li, J.: Ice thickness and bed map for Jakobshavn Isbræ, CReSIS Tech. Rep., 2008-1, 2008.

Raney, K.: IceBridge PARIS L2 Ice Thickness, 2009, Boulder, Colorado USA, NASA Distrib. Act. Arch. Cent. Natl. Snow Ice Data Center, Digital media, available at: http://nsidc.org/data/irpar2.html (last access: 1 March 2013), 2009.

Robin, G. Q., Evans, S., and Bailey, J. T.: Interpretation of Radio Echo Sounding in Polar Ice Sheets, Philos. T. R. Soc. Lond., 265, 437–505, 1969.

ESSDD
7, 129–148, 2014

Ice thickness and bed topography, West Greenland

K. Lindbäck et al.

Sole, A., Payne, T., Bamber, J., Nienow, P., and Krabill, W.: Testing hypotheses of the cause of peripheral thinning of the Greenland Ice Sheet: is land-terminating ice thinning at anomalously high rates?, The Cryosphere, 2, 205–218, doi:10.5194/tc-2-205-2008, 2008.
Sole, A., Nienow, P., Bartholomew, I., Mair, D., Cowton, T., Tedstone, A., and King, M. A.: Winter motion mediates dynamic response of the Greenland Ice Sheet to warmer summers, Geophys. Res. Lett., 40, 3940–3944, doi:10.1002/grl.50764, 2013.
Stolt, R. H.: Migration by Fourier Transform, Geophysics, 43, 23–48, 1978.
Waite, A. and Schmidt, S.: Gross Errors in Height Indication from Pulsed Radar Altimeters Operating over Thick Ice or Snow, Proc. IRE, 12, 1515–1520, 1962.
van de Wal, R. S. W., Boot, W., van den Broeke, M. R., Smeets, C. J. P. P., Reijmer, C. H., Donker, J. J. A., and Oerlemans, J.: Large and Rapid Melt-Induced Velocity Changes in the Ablation Zone of the Greenland Ice Sheet, Science, 321, 111–113, doi:10.1126/science.1158540, 2008.
van de Wal, R. S. W., Boot, W., Smeets, C. J. P. P., Snellen, H., van den Broeke, M. R., and Oerlemans, J.: Twenty-one years of mass balance observations along the K-transect, West Greenland, Earth Syst. Sci. Data, 4, 31–35, doi:10.5194/essd-4-31-2012, 2012.
Welch, B. C., Pfeffer, W. T., Harper, J. T., and Humphrey, N. F.: Mapping subglacial surfaces of temperate valley glaciers by two-pass migration of a radio-echo sounding survey, J. Glaciol., 44, 164–170, 1998.
Wingham, D. J., Siegert, M. J., Shepherd, A., and Muir, A. S.: Rapid discharge connects Antarctic subglacial lakes, Nature, 440, 1033–1036, doi:10.1038/nature04660, 2006.
Wright, A. P., Siegert, M. J., Le Brocq, A. M., and Gore, D. B.: High sensitivity of subglacial hydrological pathways in Antarctica to small ice-sheet changes, Geophys. Res. Lett., 35, L17504, doi:10.1029/2008GL034937, 2008.

ESSDD
7, 129–148, 2014

Table 1. Radar system parameters for each dataset.

	UU	DTU	IceBridge
Frequency (MHz)	2.5	60	194
Peak power (W)	35	600	500
Bandwidth (MHz)	7	4	10
Pulse repetition frequency (Hz)	1000	0–32 000	9000
Sampling frequency (Hz)	1000	3.125	111
Range resolution (m)	18.8	21	4.5

ESSDD
7, 129–148, 2014

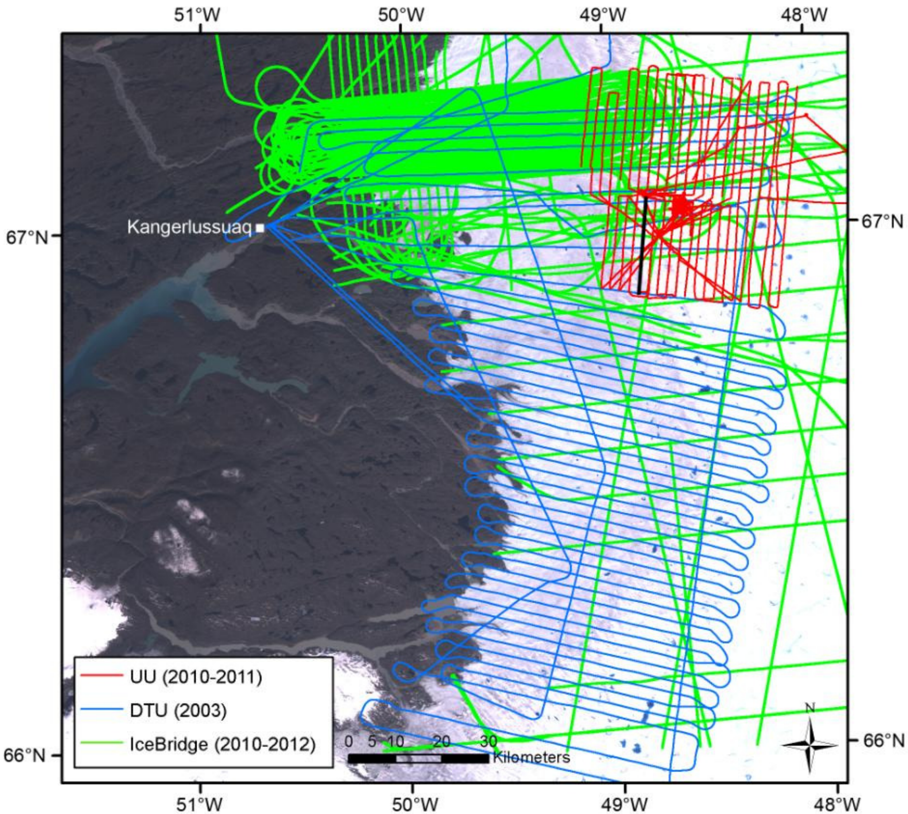

Fig. 1. Data sources consisting of ground-based radar surveys (UU dataset) and airborne surveys (DTU and IceBridge datasets) collected between 2003 and 2012. The town of Kangerlussuaq is also marked on the map. The black line in the UU dataset indicates the location of the profile in Fig. 2.

ESSDD
7, 129–148, 2014

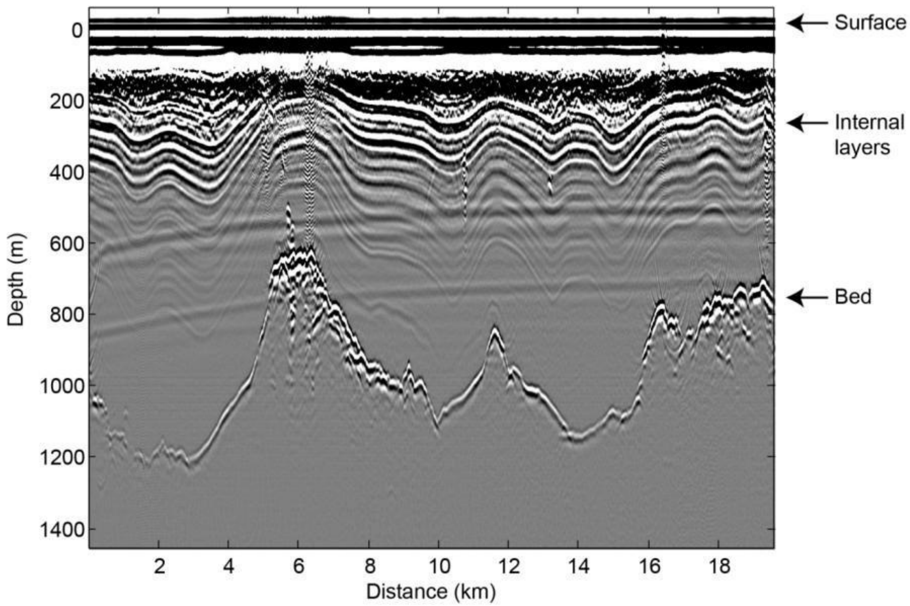

Fig. 2. An example of a processed radar image of the UU dataset, going from north to south. The location of the profile is marked in Fig. 1. Various features are indicated in the map, such as internal layers, the bed reflector with high subglacial peaks and the surface reflector.

ESSDD
7, 129–148, 2014

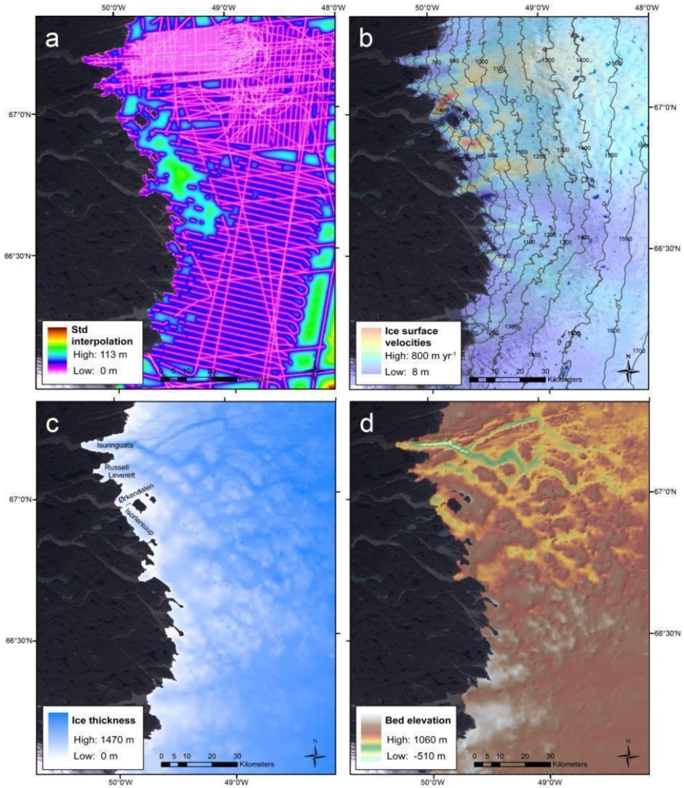

Fig. 3. (a) Data quality map showing the standard deviation of the interpolation. **(b)** GIMP surface elevations as height above the WGS-1984 ellipsoid (contours) and ice surface velocities (colour scale) from Joughin et al. (2010). **(c)** Ice thickness. Outlet glacier names are indicated in the map. **(d)** Bed elevation as height above the WGS-1984 ellipsoid. The background image is LANDSAT TM from 9 July 2001.

ESSDD
7, 129–148, 2014
Ice thickness and bed topography, West Greenland
K. Lindbäck et al.